Design of Unlicensed Dual Band Quasi-Yagi Antenna Using Semi-Bowtie for Indoor Wireless Power Transfer Application

Mohd Hezri Abdullah[1], Arjuna Marzuki[2], and Mohd Tafir Mustaffa[1]
[1] School of Electrical and Electronic Engineering, Universiti Sains Malaysia, Penang 14300, Malaysia
[2] School of Science and Technology, Wawasan Open University, Penang 10050, Malaysia
Email: hezri@student.usm.my; arjunam@wou.edu.my; tafir@usm.my

Abstract —This paper focuses on antenna for harvesting energy from a dedicated transmitter. The potential novel quasi-Yagi antenna with semi-bowtie driven element can be used as part of rectenna due to its characteristic of having directional properties and considerably wide bandwidth covering the Industrial, Scientific, and Medical (ISM) band consists of 863-870 MHz band and 902-928 MHz band. The modified quasi-Yagi is designed on a low-cost FR4 substrate with a physical size of 130 x 100 mm^2 equivalent to 0.35λo x 0.27λo. The antenna has a peak directivity of 2.7 dBi and peak gain of 2.2 dBi in the targeted unlicensed bands with bandwidth of 14.4% for the range between 0.820-0.944 GHz. The shift in the resonant frequency is achieved by varying the phase shifter length and maintaining the same width for consistency. The antenna's operating frequency range varies between 0.8 GHz until 1 GHz which is less than 1 GHz by using semi-bowtie as driven element with a specific 7.22° flare angle. The phase shift arm length of the antenna has been studied and simulated by using Computer Simulation Technology (CST) software and verified by using analytical equations. The simulated results are in accordance with the results obtained using analytical method. The same antenna geometry except variation in phase shifter arm length has been used throughout the study for consistency. The proposed antenna is promising to be used as part of rectenna for powering power management chip such as BQ25570 in a smart house environment operating at the indicated ISM bands.

Index Terms—Bowtie driver, microstrip to coplanar, sensor, rectenna, quasi-Yagi antenna

I. Introduction

Various antennas are being designed worldwide for Wireless Power Transfer (WPT) and Energy Harvesting (EH). Both types of applications need different types of antennas. For example, the energy harvesting antenna requires omnidirectional radiation [1] and has circularly polarized properties. On the other hand, wireless power transfer application requires an antenna with high directivity [2].

EH and WPT provide a green and sustainable solution for myriads of wireless applications. The EH and WPT involve absorbing ambient energy and dedicated power from transmitter respectively and converting it into electricity to power up typically low-powered sensors. Variety sources of ambient energy are wind energy, solar energy, electromagnetic energy, thermal energy, mechanical energy, tidal energy, and numerous others [3].

However, most energy sources cannot provide power for 24 hours a day except electromagnetic energy.

As such, this paper will focus on antenna technology to be used at a receiver for powering power management chip connecting to various types [4], [5] of sensors. The antenna is the receiving part of a rectenna. The antenna combined with a rectifier is known as a rectenna. The rectenna can be used in an indoor environment for application such as smart home [6].

However, most antennas will encounter the problems of interference and multipath fading, which degrades system performance. Therefore, a directional antenna, which has a considerable high gain and directivity shall be deployed.

The quasi-Yagi antenna is one of directional or end-fire antennas type. Presently these end-fire antennas are also employed in many other applications such as in point-to-point communication [1], personal area network [7], [8] and radar applications [9].

Unfortunately, the quasi-Yagi antenna exhibits narrow bandwidth, restricting its applications. Recently, some wideband quasi-Yagi antennas have been proposed in some literatures. These antennas used various methods for increasing bandwidth such as using a unique driver dipole i.e. a combination of a rectangular dipole and an elliptical dipole [10] using slots [5], [11], decreasing separation distance between the parasitic element and driven element [6], [12]. However, these antennas are either need quite a complex balun or use complex driven element shape [7], [12]. The complex geometry of the balun or driven element is found to be contributing to a bigger size antenna as well as difficult to be manufactured.

Many balun transform structures have been proposed in the published literatures to ensure the unbalanced signal is transformed into a balanced signal [13].

For example, antennas fed by coplanar waveguide is presented in [5], [9], [10]. However, deterioration of

Manuscript received August 25, 2021; revised November 18, 2021.
This work was supported by Education Ministry of Malaysia, FRGS-203/PELECT/6071417.
Corresponding author email: tafir@usm.my.
doi:10.12720/jcm.16.12.535-544

electrical performance is inevitable due to the unbalanced feed for the quasi-Yagi antenna's driver dipole. The scenario will also cause the deterioration of its radiation pattern as well as its bandwidths. As an alternative, a complex driven element geometry is used to obtain the wideband performance [7], [12].

Other types of baluns are such as coaxial probe [14], stripline [15], microstrip to CPS (coplanar stripline) transition [12], [16], coplanar width (CPW) to CPS transition [9], [17], microstrip line coupled to slot line [8] [18], [19] and so on.

There are previous literature on designing planar quasi-Yagi antennas, but the studies focused on higher than 1 GHz frequency band [10], [12], [13], [16], [20].

This paper's main objective is to study the quasi-Yagi antennas with different length of its phase shifter. The designed resonance frequencies shall be between 0.8 GHz and 1 GHz .

Quasi-Yagi antennas are studied in this manuscript for operating at frequency band between 0.8 GHz until 1 GHz, which contains ISM 868 MHz band and 915 MHz . Both bands are unlicensed bands which are suitable to be used for indoor wireless power transfer system. The planar quasi-Yagi antenna is also selected due to its high directivity, ease of fabrication, compactness dimension, and broadband characteristics of travelling-wave radiator [21]. The designed antenna shall be dual band and operates at ISM band of 863-870 MHz and 902-928 MHz.

This paper is divided into four sections, starting with introducing some of the antenna designs based on previous literatures. In Section II, a modified quasi-Yagi antenna is designed using analytical method and uses semi-bowtie as driven elements. In Section III, the simulation results of the antenna are shown and variation in phase shifter length dimensions have been studied. The analysis of antenna results as well as recommendations are also discussed in the section. The last section presents the main conclusions of the paper.

II. Antenna Structure and Analysis

A Yagi-Uda antenna consists typically of a driven element, reflector, and one or more parasitic elements. Theoretically, a quasi-Yagi antenna is a type of directive radiating structure consists of an active element, a group of passive elements, and a reflector. A Yagi-Uda antenna aims to steer the radiation to a specific direction [22]. An FR4 as a low-loss substrate is used in this work with substrate thickness, h = 1.60 mm, loss tangent of tan δ = 0.0027 and relative permittivity of εr = 4.6.

In this paper, the driven element is a semi-bowtie shape due to that the shape can create a reasonable wide bandwidth as required. A basic solid semi-bowtie antenna is shown in Fig. 1.

Fig. 1 shows the basic structure of a semi-bowtie antenna. Theoretically, the design procedure of a rectangular microstrip patches and printed bowtie is same. However, there is a modification being done on the equations of the rectangular patches in [22] for producing a set of equations for microstrip bowtie antenna as in [23]. The equation for microstrip bowtie antenna has been further modified in this manuscript for being used with microstrip semi-bowtie antenna. The modified equations are as below:

$$W_{im} = (\frac{(W/2)+Wc}{2}) \quad (1)$$

$$\varepsilon_{effm} = \left(\frac{\varepsilon_r+1}{2}\right) + (\frac{\varepsilon_r-1}{2})(1+12h/W_{im})^{-0.555} \quad (2)$$

W_{im} represents the effective modified width. The $\frac{W}{2}$ represents the semi-bowtie width as in Fig. 1 and ε_{effm} is the modified effective permittivity for semi-bowtie. Wc is the minor width as in Fig. 1, ε_r is the relative permittivity of the substrate. h is the substrate thickness.

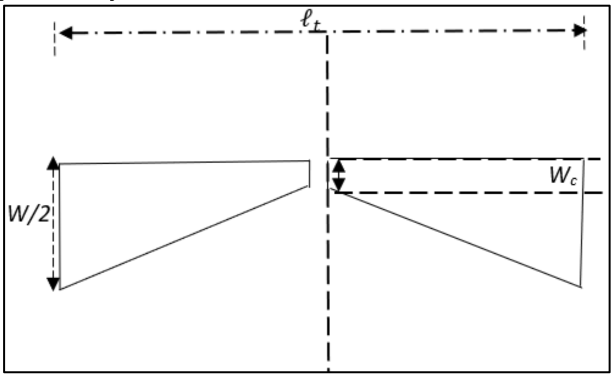

Fig. 1. The structure of a semi-bowtie antenna with dimensions.

The equations used for the semi-bowtie antenna are as below:

The (1) and (2) have been used in the below modified equations.

Total length of semi-bowtie driven element, ℓ_t

$$\ell_t = \frac{c}{2fr\sqrt{\varepsilon_{effm}}} \quad (3)$$

$$\ell_{im} = \frac{\lambda_g}{4} \quad (4)$$

where λ_g equals dielectric wavelength, f_r is the resonant frequency and ℓ_{im} is the phase shift arm length of quasi-Yagi semi-bowtie antenna. The ℓ_{im} also represents L_{p1} and L_{p2} as in Fig. 3.

$$\lambda_g = \frac{\lambda_\circ}{\sqrt{\varepsilon_{effm}}} \quad (5)$$

where $\lambda_\circ$ is the wavelength in free space and c is speed of light and f_r is the resonant frequency.

$$\lambda_0 = \frac{c}{fr} \quad (6)$$

The semi-bowtie shape antenna is related with phase shifter length by referring (1) until (7).

The definition of $\frac{\lambda_g}{4}$ in this work is as below:

$$\frac{\lambda_g}{4} = Lp1 - Lp3 = \text{phase shift arm} \quad (7)$$

Note: *Lp1=Lp2*

In short, the phase shift arm length used can be predicted by using the above equations.

In this design, flare angle @ θ is fixed at ~ 7.22° due to the angle is best suited for semi-bowtie design at both the indicated ISM bands. The flare angle is obtained by using the equation in [13].

In addition, the semi-bowtie width $\frac{W}{2}$ is directly proportional to the flare angle.

A. Phase Shifter

Various phase shifters exist such as transmission line phase shifters, semiconductor device phase shifters, mechanical phase shifters, and ferrite phase shifters. A transmission line phase shifter has been designed in this work due to having comparatively simpler design as compared to other type of phase shifters.

The desired phase shift can be achieved by varying the microstrip line length. In this work, the length of the phase shifter is calculated by using (7). The phase shifter function is used for changing the even to odd signal, which can be passed through via CPS to the driven element.

B. Microstrip Linefeed

Width of linefeed (W_f) is designed so that the characteristic impedance of the microstrip (50 Ω) is matched to the balanced microstrip [24].

In this paper, the height, *h* of the FR4 substrate thickness used is 1.6 mm with a relative dielectric constant εr = 4.6, loss tangent tan δ = 0.02 [25], [26], as shown in Fig. 3. In this design, the width of microstrip line, W_f as in Fig. 3 is found in the design by using the equations in [16]. The microstrip linefeed and its antenna structure are simulated by using CST [27].

On the other hand, coplanar stripline (CPS) lines are the balanced lines used for feeding balanced antennas like dipole and bowtie [21], [23]. CPS lines are also used as microwave components like balanced mixers, and so on. A comprehensive analysis technique of the CPS lines is given in [28].

In this work, the quasi-Yagi antenna is designed with phase shifter and ground for controlling the antenna's directivity. The combination of microstrip to CPS feedline is used in this work compared to a more simplified differential CPS. The usage of CPS will normally degrade the antenna performance due to generating multiple harmonics order. However, the higher-order modes can also contribute to increasing the antenna's bandwidth .

C. Antenna Geometry

The proposed quasi-Yagi antenna of size 130×100 mm^2 is designed on a low-cost FR4 substrate as shown in Fig. 3. It is made of semi-bowtie as driven element, microstrip-to-CPS transition and another semi bowtie as a parasitic director. All the components are placed on top of a substrate. A truncated ground plane with a dimension of $Wg \times Lg$ is designed at the bottom of the substrate. It functions as a reflector. The antenna has metallization on the top of the driven elements, director elements and microstrip to CPS feed. The bottom side has metallization on the truncated ground plane, which is used as a reflector element. The microstrip-to-CPS transition [12], [16], [21], [23] are used to feed the antenna. The microstrip-to-CPS transition consists of a linefeed, asymmetric T-junction as phase shifter and CPS are used for feeding semi-bowtie driven element using similar concept to the recent studies in [12], [16]. The asymmetric T-junction is used as a phase shifter for supplying 180° phase delay and generates the odd mode at centre frequency of 0.868 GHz, and 0.915 GHz. As a result, the phase shifter can transform an unbalanced input signal to become a balanced signal at the semi-bowtie driven element. Hence, the driven element will radiate the signal at the unlicensed bands in case of the antenna is designed as transmitter.

Initially, the microstrip-to-CPS transition has been designed at three different resonance frequencies of 915 MHz, 868 MHz and 807 MHz respectively. Then the best design with resonance frequency of 868 MHz has been chosen due to it can operate in dual band mode of the indicated ISM bands.

The evolution of the design is as in Fig. 2. It shows the steps taken in designing the antenna. For stage (a), a truncated ground is placed at the back side. In stage (b), the line feed, balun and coplanar have been tested for getting the required even to odd signal. Initially a conventional quasi-Yagi has been designed in stage (c) and the design is further improved in stage (d) for getting a better directivity and gain. Stage (e) helps in increasing the bandwidth but the radiation pattern slightly deviates from mainlobe direction. Finally, the sufficient bandwidth and unidirectional mainlobe which can cover both unlicensed bands have been obtained by tuning the phase shift arm length as in stage (f). The evolution of the design has been done as in Fig. 2 and later simulated and optimized by using CST software.

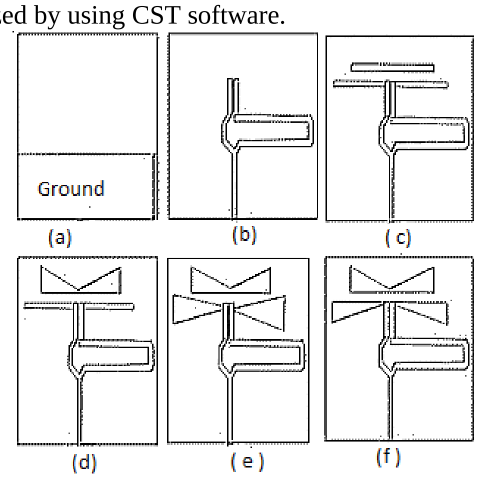

Fig. 2. The design steps (progress) of the proposed antenna: (b) Antenna 1, (c) Antenna 2, (d) Antenna 3, (e) Antenna 4 , (f) Antenna 5 and (proposed structure). All views belong to the front side while back sides of all antennas are same with Fig. 2(a).

Fig. 3 shows the antenna geometry. The antenna uses two semi-bowtie as driven elements. A parasitic element with a semi-bowtie shape is used as a director.

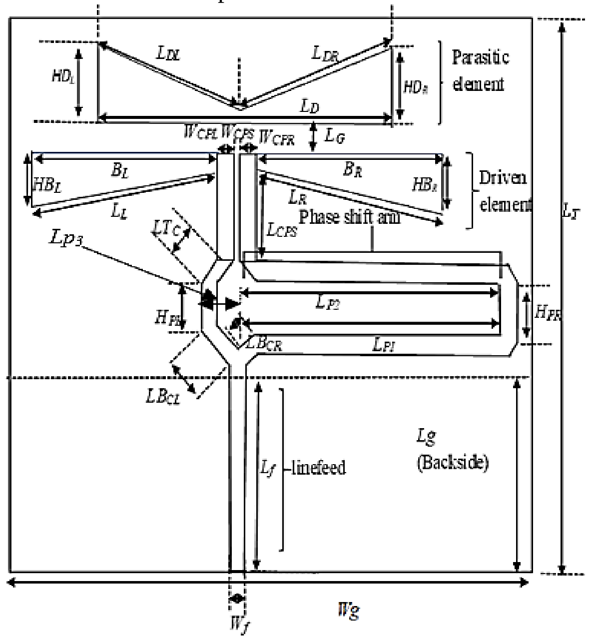

Fig. 3. The modified quasi-Yagi is designed by using semi-bowtie as a driven element.

TABLE I: FINALIZED PARAMETERS USED IN FIG. 3

Variable	Value (mm)	Variable	Value (mm)
L_{DL}	42.5	L_{p2}	50.0
L_{DR}	42.5	LB_{CR}	6.50
L_D	85.0	L_{P1}	50.0
HD_L	8.60	H_{PR}	8.00
HD_R	8.60	H_{PL}	6.70
W_{CPS}	0.50	LB_{CL}	6.50
L_G	58.0	L_f	58.0
L_{CPSR}	8.00	W_f	3.30
L_T	100.0	W_{CPR}	2.00
B_L	47.8	LT_{CL}	6.60
HB_L	7.00	LB_{CR}	5.60
L_L	43.5	W_{CPL}	2.00
HB_R	7.00	W_g	130.0
L_R	43.5	B_R	47.8
Lp3	6.60	LDD	3.65

Note:
Flare angle (θ_0) is ~ 7.22 degrees has been used throughout the design for consistency.

The antenna is studied because theoretically the resonant frequency *(fr)* and its radiation efficiency can be controlled by varying its phase shifter arm length. A quasi-Yagi with bowtie director can improve the bandwidth by 240% compared to a typical quasi-Yagi antenna using a straight director by controlling its flare angle (θ_0) [19].

In this work, an expected considerably larger bandwidth from less complex in terms of the quasi-Yagi antenna's geometry with a reasonable gain is studied. The antenna is designed at the centre frequency of 0.868 GHz by using (1) until (7). Even though the design frequency used is designed at centre frequency of 0.868 GHz, its expected bandwidth is expected to be covering both the centre frequency 0.868 GHz and 0.915 GHz . This is significance because by using a single antenna, two ISM bands can be covered. The antenna design is a challenge because the same geometry is used for covering both frequency bands .

This manuscript predicts that the usage of semi-bowtie driven element with specific phase shifter arm lengths and flare angle shall help ensuring the resonant frequencies are in the range between 0.8 GHz until 1 GHz. The same width of phase shift arm is used throughout the design. Generally, the resonant frequencies shall influence its gain, directivity, and mainlobe direction in E and H-plane of the modified quasi-Yagi antenna. In this design, the effects are more dominant since semi-bowtie is used as driven element instead of ordinary dipole. The full bowtie is not preferred in this design because its big flare angle will cause the resonant frequencies to move to different centre frequencies. The variation in driven element and phase shift arm shall help in shifting the resonant frequencies in the specified range as required. The properties shall be explored further in terms of its reflection coefficients, E-plane and H-plane radiation pattern, gain, directivity, and numerous others.

In this work, the total optimal length for the driven element is calculated using (3) and is expected to be slightly differ from the $\frac{\lambda_g}{2}$ in vacuum due to the antenna is printed on a dielectric substrate. Generally, the dielectric constant directly affects the driven element length in terms of loading effect [24], [25]. The optimized parameters are shown in Table I.

III. RESULTS

A. Results

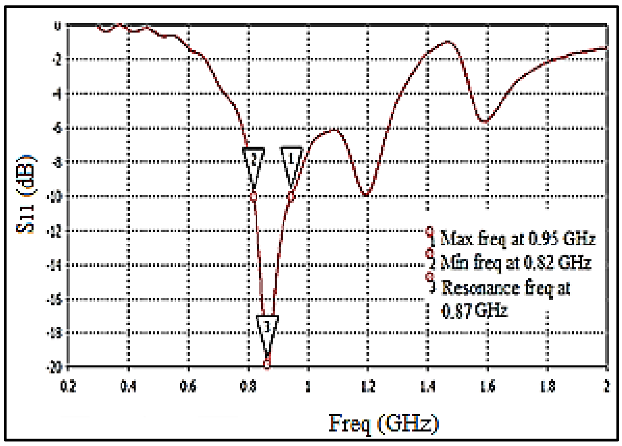

Fig. 4. Reflection coefficients (S_{11}) vs. Frequency at resonance frequency of 0.866 GHz and its bandwidth covers the ISM band 0.915 GHz and ISM 868 GHz using semi-bowtie as the driven element.

Fig. 4 shows the reflection coefficients (S_{11}) of the antenna at centre frequency of 0.868 GHz. Its phase shift arm lengths are within the range for obtaining the ISM centre frequency of 0.915 GHz and 0.868 GHz simultaneously by using a single antenna. All the parameters are as in Table I. The selection is done by considering its reflection coefficients, bandwidth and radiation pattern.

A longer phase shift arm length is tested at 53.1 mm and the length has shifted the resonant frequency to 0.821 GHz as well as having a narrower bandwidth. Its polar radiation pattern diagram is as in Fig. 5. The radiation pattern is not in unidirectional direction.

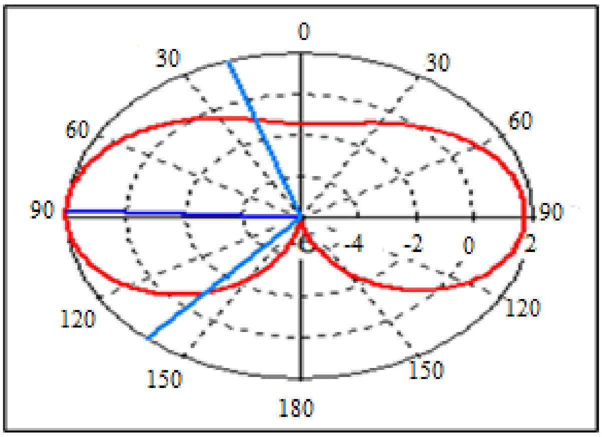

Fig. 5. Polar diagram of resonant frequency 0.821 GHz with phase shift arm length equals 53.1 mm in H-plane (phi = 90°)

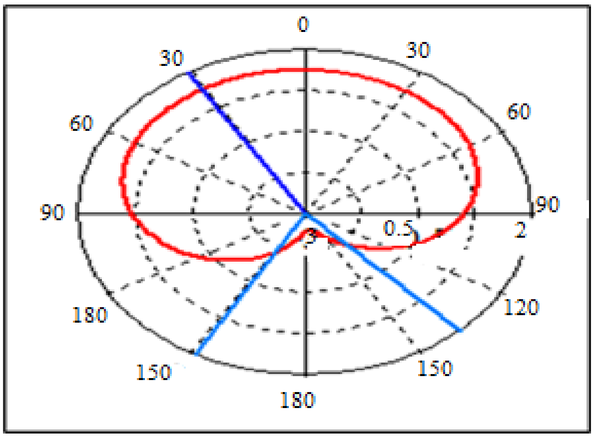

Fig. 6. Polar diagram at resonant frequency of 0.887 GHz with phase shift arm length equals 48 mm in H-plane (phi = 90°).

At phase shift arm length of ~ 48 mm as in Fig. 6, the resonance frequency is at 0.887 GHz with lower frequency of 0.838 GHz and its upper frequency was 0.952 GHz. The radiation is unidirectional. Fig. 6 shows its polar diagram and Fig. 7 shows its reflection coefficients.

At phase shift arm ~ 46 mm, the resonance frequency is at 0.916 GHz. The bandwidth does not cover the ISM 863-870 MHz band and just covers 915 MHz band as can be observed in Fig. 7. At phase shift arm ~ 51.8 mm, the resonance frequency is 0.887 GHz, lower frequency at 0.839 GHz and upper frequency at 0.953 GHz. The radiation is unidirectional and Fig. 7 shows its reflection coefficients. As such, the optimum phase shift arm of the range 48 mm until 52 mm are used for getting the dual band characteristics as in Fig. 7.

The bandwidth is influenced by the flare angle (θ_0) of the semi-bowtie. The same θ_0 of 7.22° is used throughout the study of the antenna for consistency. Multiple higher modes are observed in Fig. 4 and Fig. 7 due to the use of coplanar stripline (CPS) for feeding the driven. The use of CPS is similar to the one used in [12], [16]. However, the multiple modes are weak due to they have been minimized by optimizing the dimensions of coplanar stripline.

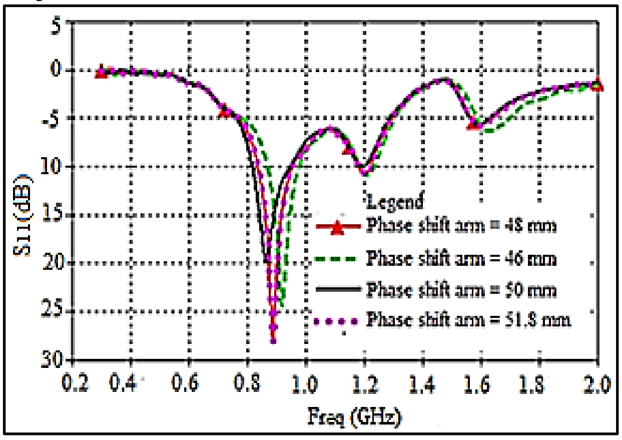

Fig. 7. Reflection coefficient at resonant frequency of 0.868 GHz with different phase shift arm lengths.

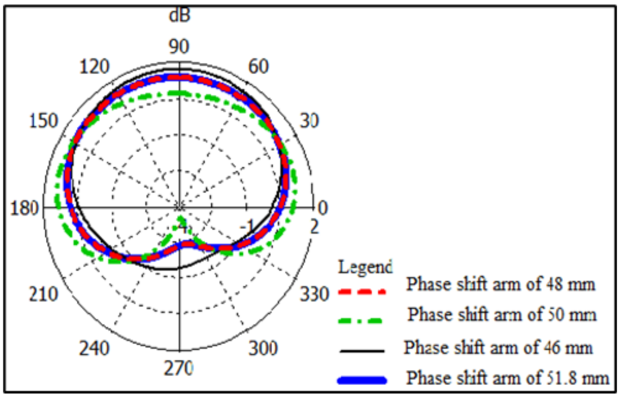

Fig. 8. Polar diagram at resonant frequency of 0.868 GHz with different phase shift arm lengths in H-plane (phi = 90°)

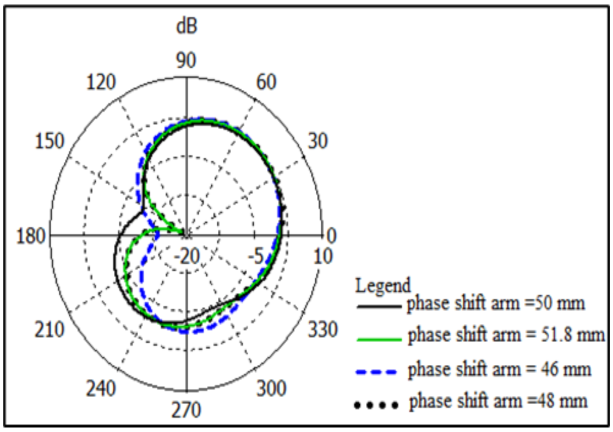

Fig. 9. Polar diagram at resonant frequency of 0.868 GHz with different phase shift arm lengths in E-plane (phi = 0°)

In a scenario whereby the semi-bowtie width is less than the designed 7 mm, the S_{11} will be worse. In Fig. 3, the width of semi bowtie used is 7 mm. The 7 mm width is critical due to the value has been used in (1) until (7) for gaining the length of driven element and phase shift arm of the antenna at the selected frequencies.

Fig. 8 and Fig. 9 show the 2D radiation pattern of the resonant frequencies designed at 0.868 GHz in H-plane and E-plane respectively. Fig. 8 indicates that the H-plane radiation pattern is in the unidirectional direction and the pattern is almost the same for all the selected phase shift arm lengths.

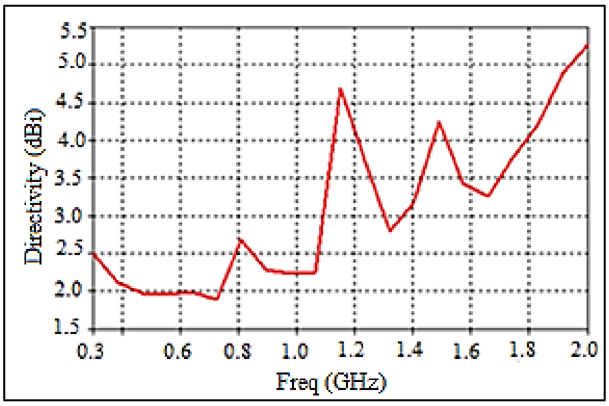

Fig. 10. Graph of directivity vs frequency for resonant frequency at 0.868 GHz.

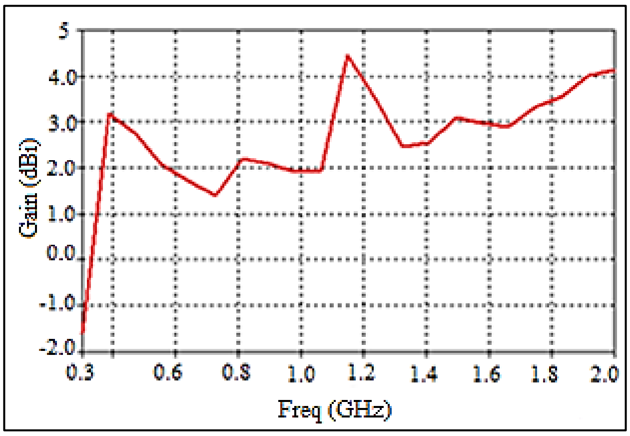

Fig. 11. Graph of Gain vs Frequency for resonant frequency at 0.868 GHz.

Fig. 9 shows the E-plane scenario where the the selected phase shift arm lengths have almost the same radiation pattern. Based on Fig. 8 and 9, the proposed quasi-Yagi has a mainlobe magnitude of 1.37 dB in the H-plane and in E-plane is 2.3 dB. This indicates that the antenna can ensure the radiation pattern has a high unidirectional radiation in E and H-plane at both ISM bands. The antenna is not symmetrical in physical due to the balun arms which create the 180° phase shift for a signal from the microstrip line to coplanar line. The asymmetry geometry produces a mild deviation for the mainlobe of the radiation pattern [12], [16]. Fig. 10 reveals that the directivity of the antenna varies with frequencies. The variation in directivity between 0.8 GHz until 1 GHz is between 2.7 dB and 2.3 dB. Even though, the directivity is higher at 1.17 GHz but its radiation pattern is not unidirectional. As such, a lower region of directivity is preferred at between 0.8 GHz until 1 GHz for a better radiation pattern as in Fig. 10 and Fig. 11. The gain was stable at about 1.9 dB until 2.2 dB for the specified range of 0.8 GHz until 1 GHz. In other words, both ISM bands are well covered by the antenna.

B. Discussions

The change in resonant frequency (*fr*) of the quasi-Yagi antenna depends on the lengths (i.e., *Lp1* and *Lp2*) of the phase shifter as well as both driven elements (B_R and B_L) [27] while maintaining other parameters. However, in this work, the driven element is maintained at length $\frac{\lambda_g}{4}$ of the 0.868 GHz as designed frequency. This is to ensure that only phase shift arm is varied for controlling the radiation pattern, dual band properties as well the bandwidth covering both the unlicensed bands. In the meantime, its main function as a phase shifter for the input signal conversion from even to odd signal operates at its best.

The slight difference in lengths (Lp_1 and Lp_2) with respect to the analytical method occurred due to the loading effect of the substrate [24], [25] as well as the imperfection of FR4 substrate to be used at near 1 GHz band [25].

The antenna is designed at 0.868 GHz due to its phase shift arm lengths can cover the $\frac{\lambda_g}{4}$ of both the ISM 0.915 GHz and 0.868 GHz bands. The phase shift arm length of the antenna are between 48 mm and 52 mm. Therefore, a single antenna is used for covering the dual ISM band. The width of driven elements and phase shift arms do contribute to the resonant frequency of the antenna. For example, an increment of another 1 or 2 mm from the existing 2 mm width of the microstrip used at phase shift arm length leads to a jump of resonant frequency away from 0.868 GHz and 0.915 GHz bands. The scenario happens due to the change in surface current distribution in the antenna structure [23], [24], [26].

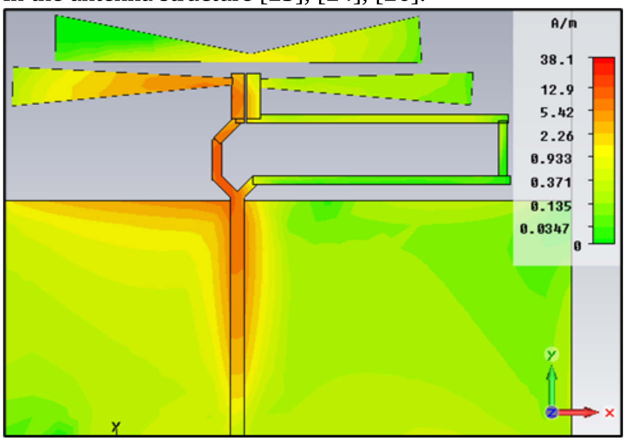

Fig. 12. Current density distribution at fundamental frequency of 0.807 GHz.

The surface current distribution at the three distinct frequencies i.e., at 0.915 GHz, 0.868 GHz and 0.807 GHz is obtained for understanding the radiation mechanism of the antenna. The outcomes of the surface current distributions are shown in Fig. 12 until Fig. 14. Fig. 12 shows the current density distribution at 0.807 GHz. The figure shows that it is mainly due to the left semi-bowtie as the surface current distribution concentrates on the left area. On the other hand, the surface current distribution at its director and right semi-bowtie are relatively lower. The situation shows that both the sides of director and the right semi-bowtie have comparatively low effect towards the radiation mechanism of the antenna at the specified frequency. The surface current distribution at 0.868 GHz and 0.915 GHz are as in Fig. 13 and Fig. 14 respectively. Both figures reveal that surface current on the ground plays a significant role in the increment of mainlobe radiation and reduction of back lobe. The phase shift arm as well as the left semi-bowtie contribute towards the radiation mechanism at both 0.868 GHz and 0.915 GHz as observed in Fig. 13 and Fig. 14. The coupling between both coplanar striplines (CPS) have helped in the radiation mechanism at both ISM frequencies such that the right semi-bowtie has fewer contribution compared to the CPS.

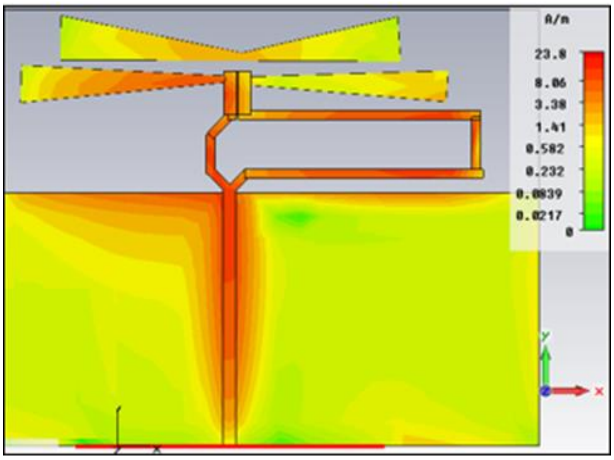

Fig. 13. Surface current distribution at resonance frequency of 0.868 GHz.

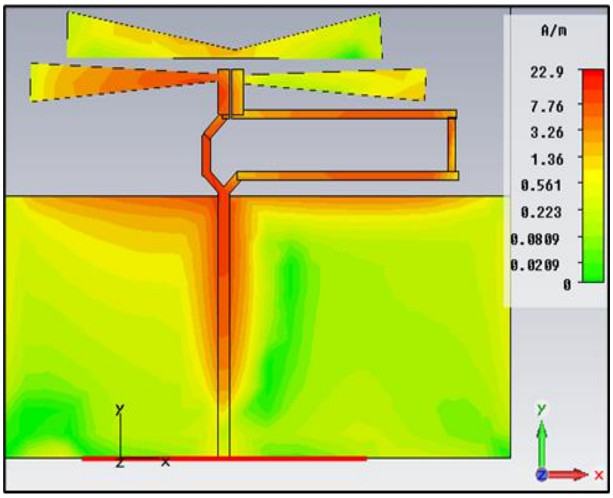

Fig. 14. Surface current density distribution at frequency of 0.915 GHz.

The semi-bowtie shape is almost like concave shape which helps in concentrating current through the shape of the driven elements [23]. In general, most of the surface current concentration happens at specific spots such as phase shift arms, left driven elements, coplanar stripline and linefeed. The semi-bowtie shape also helps in miniaturizing the antenna overall size compared to conventional quasi-Yagi using bowtie as driven element.

All in all, the (1) until (7) have shown its relevancy as a starting point for designing quasi-Yagi with semi-bowtie as driven element. In this work, further optimization of the main parameters such as phase shift arm lengths and length of driven element are done by using CST software. The results from theoretical and simulations methods are compared for consistency.

If a bowtie antenna only is used, the mainlobe direction is at the antenna's front and back and is not in the endfire direction [29].

The gain of the antenna can be further improved by loading with metamaterial [30], using a lower relative permittivity and comparatively thinner substrate [6] as well as a closer distance between director and the driven element [12], [24].

The antenna's dimensions can be further improved by shortening the microstrip feedline's length but still achieving a matching impedance value. This can be achieved by using a thicker substrate [31] or changing the line feed geometry [10]. A λ/4 transformer [12], [16] method can be used for the quasi-Yagi antenna even though it increases the linefeed complexity. The comparison of single-type microstrip antennas performance are shown in Table II.

TABLE II: ANTENNA PERFORMANCE COMPARISONS

Ref.	Electrical size	Gain (dBi)	Max. Bandwidth (GHz)
[10]	0.5 λo x 0.38 λo	>4	3.75 - 10.4
[11]	0.46 λo x 0.39 λo	2.38	5.35 - 5.52
[12]	0.36 λo x 0.38 λo	6 - 7.7	1.71 - 1.9
[13]	0.48 λo x 0.35 λo	5.0 - 6.8	1.606 - 3.07
[15]	0.41 λo x 0.28 λo	NM	2.07 - 2.71
[16]	0.46 λo x 0.46 λo	4.8	9 - 12.5
[24]	0.43 λo x 0.33 λo	5.6	0.428 - 0.50
This work	0.35 λo x 0.27 λo	1.9 - 2.2	0.82 - 0.95

*NM = Not mentioned

IV. CONCLUSION

A novel dual-band modified quasi-Yagi antenna with semi-bowtie as driven element has been designed. It has a unidirectional radiation pattern in E and H-plane and can achieve a comparatively wide bandwidth of 14.4% which is bigger than [11] and [12] while its electrical size is smaller than antennas in [10], [13], [15], [16] and [24]. The bandwidth shall not be too big due to it will interfere with other licensed bands. This antenna has the benefit of capability for covering both the Industrial, Scientific, and Medical (ISM) consists of 863-870 MHz band and 902-928 MHz band at a smaller electrical size compared to the previous literatures. Most of antennas in Table II are designed at frequencies above 1 GHz. In this work, the designed antenna has a peak directivity of 2.7 dBi and peak gain of 2.2 dBi in both unlicensed bands. The antenna characteristics suits well to be used as part of rectenna for indoor wireless power transfer application.

In this design, the resonant frequency, $f_{r,}$ of the antenna depends largely on the type of driven element, the phase shift arm length as well as the width of the microstrip line. The modified equations of (1) until (7) have helped to predict the required lengths of phase shift arms as well as the driven element. This is because the equations are based on the dimension of semi-bowtie as driven elements. The equations are specifically can be used as a starting point for getting the initial parameter designs of the quasi-Yagi with semi-bowtie as driven element.

This paper shows that the antenna is flexible because it can operate simultaneously in the indicated dual ISM bands. The semi-bowtie as driven element together with phase shift arms have helped in creating the dual bands. The use of a semi-bowtie-driven element with a flare angle of 7.22 degrees in the antenna has contributed to controlling the operating frequency between 0.8 GHz and 1 GHz. The specified dimensions of phase shifter arm length have helped in tuning the resonant frequency and the mainlobe direction. Hence, the antenna is suitable to be used as part of rectenna for powering power management chip in a smart houses or smart cities due to its unidirectional properties as well as comparatively smaller sizes compared to the previous literatures.

Conflict of Interest

The authors declare no conflict of interest.

Author Contributions

All the authors involved in producing the paper and approved the final version.

Acknowledgement

The authors wish to thank the department of Electrical and Electronic Engineering of Universiti Sains Malaysia for the provided expertise. This work was supported by Education Ministry of Malaysia, FRGS-203/PELECT/6071417.

References

[1] S. D. Assimonis, S. N. Daskalakis, and A. Bletsas, “Sensitive and efficient RF harvesting supply for batteryless backscatter sensor networks,” *IEEE Trans. Microw. Theory Tech.*, vol. 64, no. 4, pp. 1327–1338, Apr. 2016.

[2] J. Janhunen, K. Mikhaylov, J. Petäjäjärvi, and M. Sonkki, “Wireless energy transfer powered wireless sensor node for green IoT: Design, implementation and evaluation†,” *Sensors (Switzerland)*, vol. 19, no. 1, pp. 1-22, Dec 2019.

[3] K. S. Divakaran, K. Deepti, and Nasimuddin, “RF energy harvesting systems: An overview and design issues,” *Int. J. RF Microw. Comput. Eng.*, vol. 29, no. 1, pp. 1-15, Jan. 2019.

[4] M. Cansiz, D. Altinel, and G. K. Kurt, “Efficiency in RF energy harvesting systems: A comprehensive review,” *Energy*, vol. 174, pp. 292–309, May 2019.

[5] Q. Awais, Y. Jin, H. T. Chattha, M. Jamil, H. Qiang, and B. A. Khawaja, “A compact rectenna system with high conversion efficiency for wireless energy harvesting,” *IEEE Access*, vol. 6, pp. 35857–5866, Jun.2018.

[6] S. Keyrouz, “Practical rectennas: Far-field RF power harvesting and transport,” Ph.D. dissertation, Faculty Electrical Engineering, Eindhoven University of Technology, Eindhoven, The Netherlands, 2014.

[7] M. Sun, X. Qing, and Z. N. Chen, “60-GHz end-fire fan-like antennas with wide beamwidth,” *IEEE Trans. Antennas Propag.*, vol. 61, no. 4, pp. 1616–1622, Apr. 2013.

[8] L. Pazin and Y. Leviatan, “A compact 60-GHz tapered slot antenna printed on LCP substrate for WPAN applications,” *IEEE Antennas Wirel. Propag. Lett.*, vol. 9, pp. 272–275, 2010.

[9] J. Shao, G. Fang, Y. Ji, K. Tan, and H. Yin, “A novel compact tapered-slot antenna for GPR applications,” *IEEE Antennas Wirel. Propag. Lett.*, vol. 12, no. 19, pp. 972–975, 2013.

[10] X. Zhao, Y. Huang, X. Xue, and G. Wen, “A CPW-fed broadband quasi-Yagi antenna with low cross-polarization performance,” *AEU - Int. J. Electron. Commun.*, vol. 83, pp. 188–192, Jan. 2018.

[11] N. M. Tarpara, R. R. Rathwa, and N. A. Kotak, “Design of slotted microstrip patch antenna for 5G application,” *Int. Res. J. Eng. Technol.*, vol. 5, no. 4, pp. 2827-2832, April 2018.

[12] M. Elahi, Irfanullah, R. Khan, A. A. Al-Hadi, S. Usman, and P. J. Soh, “A dual-band planar quasi Yagi-Uda antenna with optimized gain for LTE applications,” *Prog. Electromagn. Res. C*, vol. 92, pp. 239–250, May 2019.

[13] R. Nayak and S. Maiti, “A review of bow-tie antennas for GPR applications,” *IETE Tech. Rev. (Institution Electron. Telecommun. Eng. India)*, vol. 36, no. 4, pp. 382–397, Jul. 2019.

[14] R. Chopra and G. Kumar, “Compact, broadband, and high gain directional endfire antenna,” *Microw. Opt. Technol. Lett.*, vol. 62, no. 7, pp. 2546-2553, July 2020.

[15] H. Andre, R. Fernandez, and Baharuddin, “Dipole planar bowtie printed antenna for ism application,” in *Proc. IOP Conference Series: Materials Science and Engineering*, Sep. 2019, vol. 602, no. 1, pp. 012022.

[16] B. Atabay, “Design and realization a Quasi Yagi antenna array and its feed system printed on a ceramic substrate for X-Band radar applications,” Master thesis, School of

Natural and Applied Sciences, Middle East Technical University, Ankara,Turkey, 2019.
[17] H. K. Kan, R. B. Waterhouse, A. M. Abbosh, and M. E. Bialkowski, "Simple broadband planar CPW-fed quasi-Yagi antenna," *IEEE Antennas Wirel. Propag. Lett.*, vol. 6, pp. 18–20, 2007.
[18] K. Sun, D. Yang, S. Liu, and T. Yang, "A broadband and low cross polarization antenna with a balun of microstrip line coupling to slot line," *PLoS One*, vol. 13, no. 3, pp. e0194181, Mar. 2018.
[19] J. M. Gonzalez-Perez, L. Marnat, and A. Shamim, "24GHz paper based inkjet printed quasi Yagi-Uda antenna with new bowtie director," in *Proc. 12th European Conference on Antennas and Propagation (EuCAP 2018)*, 2018.
[20] K. Da Xu, D. Li, Y. Liu, and Q. H. Liu, "Printed quasi-yagi antennas using double dipoles and stub-loaded technique for multi-band and broadband applications," *IEEE Access*, vol. 6, pp. 31695–31702, Jun. 2018.
[21] C. E. Capovilla, H. X. Araujo, A. J. S. Filho, and L. C. Kretly, "Experimental analysis of Quasi-Yagi antenna shapes," *PRZEGL AD ELEKTROTECHNICZNY Electrical Rev.*, pp. 100-104, 2013.
[22] C. A. Balanis, *Antenna Theory Analysis and Design, 3rd ed.*. Hoboken, New Jersey, U.S, John Wiley and Sons, 2005.
[23] A. C. Durgun, C. A. Balanis, C. R. Birtcher, and D. R. Allee, "Design, simulation, fabrication and testing of flexible bow-tie antennas," *IEEE Trans. Antennas Propag.*, vol. 59, no. 12, pp. 4425–4435, August 2011.
[24] Y. Bakirli, A. Selek, and M. Secmen, "Broadband compact quasi Yagi antenna for UHF wireless communication systems with enhanced performance at UHF ISM bands," *Radioengineering*, vol. 29, no. 3, pp. 460–470, Sept. 2020.
[25] R. L. R. D. Silva, S. T. M. Gonçalves, C. Vollaire, A. Bréard, G. L. Ramos, and C. G. D. Rego, "Analysis and optimization of ultra-low-power rectifier with high efficiency for applications in wireless power transmission and energy harvesting," *J. Microwaves, Optoelectron. Electromagn. Appl.*, vol. 19, no. 1, pp. 60–85, March 2020.
[26] O. El Maleky, F. Ben Abdelouahab, M. Essaaidi, and N. Abdelfatah, "Miniature design of T-Shaped frequency Reconfigurable antenna for S-Band Application using Switching Technique," *Int. J. Electr. Comput. Eng.*, vol. 7, no. 5, p. 2426-2433, Oct.2017.
[27] W. Zhang, Y. Zhuang, C. Song, Y. Huang, and J. Zhou, "A dual-band Quasi-Yagi wearable antenna with high directivity," in *Proc. IEEE MTT-S International Wireless Symposium, IWS 2018 - Proceedings*, 2018, pp. 1–3.
[28] L. Zhu and K. Wu, "Field-extracted lumped-element models of coplanar stripline circuits and discontinuities for accurate radio-frequency design and optimization," *IEEE Trans. Microw. Theory Tech.*, vol. 50, no. 4, pp. 1207–1215, April 2002.
[29] A. Karampatea and K. Siakavara, "Synthesis of rectenna for powering micro-watt sensors by harvesting ambient RF signals' power," *Electron.*, vol. 8, no. 10, p. 1108, Oct. 2019.
[30] L. Liu, C. Zhang, Y. Liu, and Y. Hua, "A high gain and directivity bowtie antenna based on single-negative metamaterial," *J. Microwaves, Optoelectron. Electromagn. Appl.*, vol. 17, no. 2, pp. 246–259, Jun. 2018.
[31] H. N. Awl, *et al.*, "Bandwidth improvement in bow-tie microstrip antennas: The effect of substrate type and design dimensions," *Appl. Sci.*, vol. 10, no. 2, p. 504, Jan. 2020.

Mohd Hezri Abdullah was born in Kedah, Malaysia, in 1975. He received the B.Eng. degree from the University of Sheffield, UK, in 1998 and the M.Eng. degree from the Universiti Teknikal Malaysia Melaka in 2013. B.Eng is in Electronic (Communication) and M.Eng is in Electronic (Telecommunication System). He is currently pursuing the Ph.D. degree with the School of Electrical and Electronic Engineering, Universiti Sains Malaysia. Prior to that he has been working in Electronic and Telecommunication field for the past 21 years with Malaysian government and multinational companies. His research interests include antenna design, RF energy harvesting, wireless broadband technology and fibre optics.

Arjuna Marzuki graduated with B.Eng. in Electronic Engineering from University of Sheffield, MSc. from Universiti Sains Malaysia and PhD from Universiti Malaysia Perlis. He was an Associate Professor with the School of Electrical and Electronic Engineering, Universiti Sains Malaysia. He is a professional engineer registered with the Board of Engineers Malaysia and a Chartered Engineer registered with the UK Engineering Council. He is also a Fellow of the Institution of Engineering and Technology (IET). For more information, he can be contacted by email at arjunam@wou.edu.my

Mohd Tafir Mustaffa received his B. Eng degree in electrical and electronic engineering from Universiti Sains Malaysia (USM), Penang in 2000. He was awarded a master's degree (M. Eng. Sc) in computer and microelectronic engineering from Victoria University, Australia in 2005 and was officially completed his Ph.D. degree in electrical engineering specializing in radio frequency integrated circuit (RFIC) in September 2009. He served as a system engineer at Data

Acquisition System (M) Sdn. Bhd. and tutor in USM. He is now a senior lecturer at the School of Electrical and Electronic Engineering, USM, Engineering Campus. Mohd Tafir Mustaffa is a Senior Member of IEEE; actively involved with IEEE Circuits and Systems Society for the last few years as a committee member. He is the author and co-author of close to 50 technical papers in conferences and journals, book, and book chapters. He was a recipient of the IETE J C Bose Memorial Award in 2017. He is currently involved in the research of analogue IC, RFIC, and RF MEMS design.